Available online at www.sciencedirect.com
ScienceDirect
Trans. Nonferrous Met. Soc. China 28(2018) 469−486
Transactions of Nonferrous Metals Society of China
www.tnmsc.cn

Co evolutions for WC−Co with different Co contents during pretreatment and HFCVD diamond film growth processes

Xin-chang WANG[1], Cheng-chuan WANG[1], Wei-kai HE[2], Fang-hong SUN[1]

1. State Key Laboratory of Mechanical System and Vibration, School of Mechanical Engineering, Shanghai Jiao Tong University, Shanghai 200240, China;
2. School of Physics and Technology, University of Ji'nan, Ji'nan 250022, China

Received 22 July 2016; accepted 3 March 2017

Abstract: Systematical researches were accomplished on WC−Co with different Co contents (6%, 10% and 12%, mass fraction). Based on the XPS and EDX, from orthogonal pretreatment experiments, it is indicated that the acid concentration, the time of the acid pretreatment and the original Co content have significant influences on the Co-removal depth (*D*). Moreover, the specimen temperature, original Co content and Co-removal depth dependences of the Co evolution in nucleation, heating (in pure H_2 atmosphere) and growth experiments were discussed, and mechanisms of Co evolutions were summarized, providing sufficient theoretical bases for the deposition of high-quality diamond films on WC−Co substrates, especially Co-rich WC−Co substrates. It is proven that the Co-rich substrate often presents rapid Co diffusion. The high substrate temperature can promote the Co diffusion in the pretreated substrate, while acts as a Co-etching process for the untreated substrates. It is finally found that the appropriate Co-removal depth for the WC−12%Co substrate is 8−9 μm.

Key words: HFCVD diamond film; WC−Co; Murakami-acid pretreatment; Co content; Co evolution

1 Introduction

Cemented carbides alloyed with varieties of metals (e.g., Co, Ni, Fe) have been extensively employed for producing cutting tools, drawing dies, stamping dies, valves, nozzles and some other wear-resistant components. As a typical ultra-hard coating, the diamond film deposited on the cemented carbide component using the chemical vapor deposition (CVD) technology can significantly prolong the lifespan and enhance the application effect [1−3], owing to the excellent properties.

Unfortunately, most of the alloying metals in such cemented carbides belong to the iron group, which have detrimental effects on the nucleation rate, growth rate and the adhesive strength of the CVD diamond film [4]. For the most commonly-used cobalt cemented tungsten carbide (WC−Co), many pretreatment techniques were proposed with the purpose of removing the Co element, for instance, selective Co etching by the acid [5], Murakami-acid [6,7], pulsed laser [8], plasma [9], water peening [10] and high temperature [11,12]. Some other approaches have also been developed for restraining the detrimental effect of the Co element, for example, providing additional ingredients (e.g. boron [13−15], carbon and nitrogen [16]) that will react with the Co element to form stable compounds, adding suitable diffusion barrier layers to restrict the migration of Co from the inside of the substrate to the substrate−film interface and even to the surface of the as-grown diamond film [17−20].

One of the major applications of diamond film in the mechanical engineering is acting as anti-friction and wear-resistant coating on the WC−Co cutting tool adopted for machining non-ferrous materials like aluminum alloy [21], graphite [22], hard metals [23], printed circuit board (PCB) [24] and composites [25]. The hot filament CVD (HFCVD) technology shows great practicality for the mass production of the diamond coated cutting tools, which is attributed to its advantages like the geometrical simplification, low cost, operational

Foundation item: Projects (51275302, 51005154) supported by the National Natural Science Foundation of China; Project (2015M580327) supported by the China Postdoctoral Science Foundation; Project (2016T90370) supported by the China Postdoctoral Science Foundation Special Funded Project

Corresponding author: Wei-kai HE; Tel: +86-15106990596; E-mail: sps_hewk@ujn.edu.cn; Xin-chang WANG; Tel: +86-13585748931; E-mail: wangxinchangz@163.com

DOI: 10.1016/S1003-6326(18)64680-1

convenience and the versatility [26,27].

It is known that increasing the Co content will enhance the fracture toughness of WC−Co cutting tools while decreasing the red hardness, so the Co-rich WC−Co cutting tools have been widely used under the conditions putting forward high requests for the fracture toughness, such as the small-diameter cutting tools. In order to deposit well-adhered and high-quality diamond films on Co-poor WC-Co cutting tools (Co content ≤6%), the two-step Murakami-acid pretreatment has become one of the most frequently-used pretreatment methods. While for the Co-rich WC−Co cutting tools, it is recognized that the stronger acid etchings by increasing the concentration of the acid solution or the etching time are required [28], and the higher the original Co content in the WC−Co substrate, the larger the Co content gradient in the corrosion layer. Under such conditions, if the thickness of the corrosion layer is not enough, it will be very difficult to totally avoid the Co diffusion during the deposition process of the HFCVD diamond film [29]. In other words, there must be different distributions and diffusions of the Co elements for WC−Co substrates with different Co contents in the pretreatment, nucleation and film growth processes, which are noteworthy to be studied.

It is believed that for either the untreated or the pretreated WC−Co substrates, the Co element diffusion from the inside to the surface of the substrate, and that from the film−substrate interface to the surface of as-grown diamond crystals are unavoidable at high substrate temperatures during the nucleation and growth processes of the CVD diamond film, adopting either the combustion flame CVD [30], plasma CVD [31] or HFCVD technologies [32]. DONNET et al [30] have indicated that under the circumstance of the combustion flame CVD, some spherical Co particles with a diameter of about 0.7 nm can be observed on the surface of the diamond film deposited on the untreated WC−5%Co substrate when the substrate temperature is higher than 800 °C, while when the temperature reduces to as low as 550 °C, such the spherical Co particle cannot be observed, but many Co ingredients dissolved in carbon films can also be detected by the energy dispersive X-ray (EDX). Adopting the HFCVD technology, POLINI et al [33] have found that when the substrate temperature is about 750 °C, a large number of Co-rich particles start to segregate on the pretreated WC−5.8%Co substrate surface after a few minutes of diamond growth. By contrast, at higher substrate temperature (940 °C), no clear Co-rich particles form after almost 2 h of diamond growth, but the X-ray photoelectron spectroscopy (XPS) results show that there are still some Co ingredients existing in the surface layer, while in a lower amount than that at 750 °C [33]. Moreover, the high-temperature etching pretreatment has even proved that when the untreated substrate surface is heated to a temperature as high as 940 °C, the Co content on the surface is reduced [34]. In consequence, it is supposed that in the wide temperature range that is appropriate for the diamond film growth (500−1000 °C), the Co evolutions for WC−Co substrates present significant dependencies to the substrate temperature, and some dynamic balances probably existing between the Co diffusion and the Co etching at certain substrate temperatures also require to be further studied.

In the present work, some ground WC−Co bars with different Co contents (6%, 10% and 12%) are selected as the research objects. Several series of experiments are conducted in order to systematically clarify the Co evolution during not only the Murakami-acid pretreatment, but also the deposition process of HFCVD diamond films, including the nucleation process, the growth process and a high-temperature heating process without using the carbon source.

2 Experimental

The ground bars with the same size specification (Fig. 1(a)), made of WC−Co materials with different Co contents but similar WC grain sizes (0.5−1.5 μm), are pre-molded and act as fundamental specimens in the present study. Co contents include 6%, 10% and 12% (standard values). Surface morphologies of the original specimens before treatment are presented in Figs. 1(b)−(d), which are observed by field emission scanning electron microscopy (FESEM, ULTRA55, Zeiss, Germany), showing ground surfaces with similar topographies. Besides, elementary compositions on the substrate surfaces, determined by averaging the EDX detection results at five dispersed sampling points, are also marked in the corresponding figures, proving that the specimens with clearly distinctive Co contents are indeed prepared.

The two-step Murakami-acid pretreatment method is used, the basic procedure of which includes two primary steps: 1) ultrasonically etching the specimen with the Murakami solution (definite or diluent Murakami solution, 10 g $K_3[Fe(CN)_6]$ + 10 g KOH + x mL H_2O) for T_M minutes in an ultrasonic vessel; 2) etching the specimen using the acid solution (10 mL 37% HCl + 30 mL 40% H_2O_2 (w/v) + y mL H_2O) for T_{ac} seconds. In addition, there is also another secondary step in such pretreatment method, which is to abrade the specimen with the paste comprised glycerol and diamond grits (3 μm) for removing the very loose surface layer, providing a number of nucleation sites and enhancing the nucleation density [14]. In the present study, the pretreatment parameters and Co content dependences of

the Co-removal depth (D) in the WC−Co substrate are firstly studied, using the factors and levels listed in Table 1 and the corresponding orthogonal experimental groups shown in Table 2, in order to provide database for the following preparations of specimens. The A_i (i=1, 2, 3, 4) means the average D value corresponding to the level i of each factor, and the R_j is the range.

The following nucleation, growth or heating experiments are all conducted in a home-made HFCVD apparatus. Arrangements for the specimens and the tantalum hot filaments used as the heat sources can totally refer to the previous research [35], the schematic diagram of which is also illustrated in Fig. 2. The experimental parameters are listed in Table 3. It is noted that the filament height (H) is defined as the vertical distance between the bar point and the tantalum filament (Fig. 2), and the minus representing that the filament is below the bar point. Herein, four groups of contrast experiments are accomplished:

1) The WC−Co specimens with three different original Co contents (6%, 10% and 12%) are pretreated by different procedures (mainly different T_{ac}) for obtaining the same D, and then submitted to nucleation experiments in the same duration (20 min) at different substrate temperatures (650, 800 and 950 °C). Moreover, the nucleation experiments are also conducted on corresponding untreated specimens, the results of which are compared with foregoing results.

2) Using the WC−12%Co substrate as the example, the Co evolutions in the pretreated and untreated specimens during the heating experiments are compared with each other. Moreover, such results are also compared with corresponding results in nucleation experiments in the same duration of 20 min at substrate temperatures of 650, 800 and 950 °C.

3) For the typical WC−12%Co specimens with the different D prepared by the different pretreatment procedures (different T_{ac}), the nucleation and heating

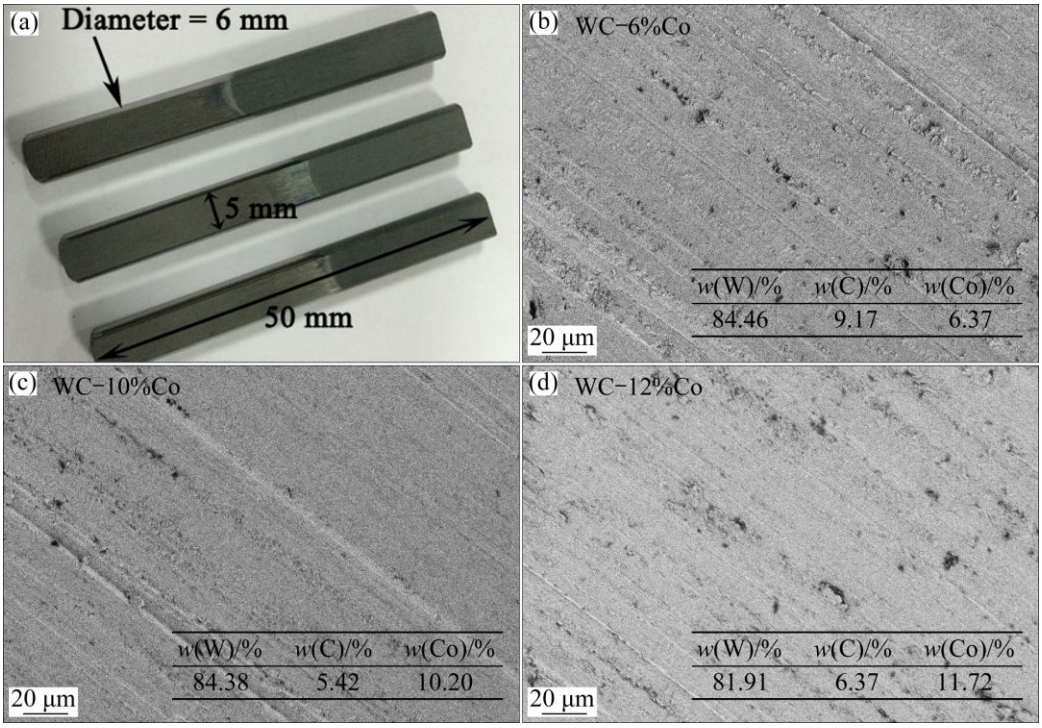

Fig. 1 Dimensions of selected WC−Co specimens (a) and surface morphologies of original WC−Co specimens without any pretreatments, together with corresponding elementary compositions on their surfaces (b−d)

Table 1 Factors and levels adopted for pretreatment parameters and Co content dependence of Co-removal depth in WC−Co substrate

Level	Volume of H_2O in diluent Murakami solution, x/mL	Murakami pretreatment time, T_M/min	Volume of H_2O in acid solution, y/mL	Acid pretreatment time, T_{ac}/s	Co content in specimen/%
1	100	15	0	30	6
2	140	20	20	15	10
3	180	25	40	45	12
4	220	30	60	60	12

Table 2 Orthogonal experimental groups for pretreatment parameters and Co content dependences of Co-removal depth in WC−Co substrate

Group No.	x/mL	T_M/min	y/mL	T_{ac}/s	w(Co)/%	D/μm
Case 1	100	15	0	30	6	8.4
Case 2	100	20	20	15	10	5.4
Case 3	100	25	40	45	12	5.2
Case 4	100	30	60	60	12	4.6
Case 5	140	15	20	45	12	6.6
Case 6	140	20	0	60	12	9.0
Case 7	140	25	60	30	10	3.6
Case 8	140	30	40	15	6	4.6
Case 9	180	15	40	60	10	5.4
Case 10	180	20	60	45	6	4.4
Case 11	180	25	0	15	12	7.2
Case 12	180	30	20	30	12	6.2
Case 13	220	15	60	15	12	2.6
Case 14	220	20	40	30	12	4.4
Case 15	220	25	20	60	6	7.8
Case 16	220	30	0	45	10	9.0
A_1/μm	5.90	5.75	8.40	5.65	6.30	
A_2/μm	5.95	5.80	6.50	4.95	5.85	
A_3/μm	5.80	5.95	4.90	6.30	5.75	
A_4/μm	5.95	6.10	3.80	6.70	5.70	
R_j/μm	0.15	0.35	4.60	1.75	0.60	

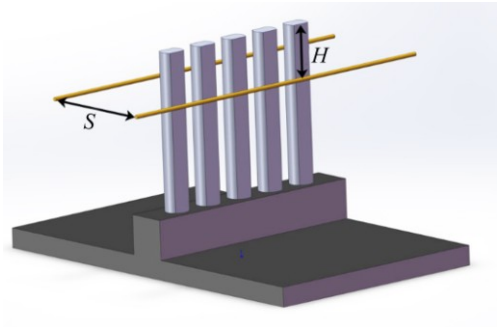

Fig. 2 Schematic diagram of arrangements for specimens and filaments

experiments in the same duration (20 min) at substrate temperature of 950 °C are also accomplished.

4) All the pretreated specimens in group 1 are also submitted to the complete deposition process of the diamond film at a definite substrate temperature of 900 °C, including a 20 min nucleation stage and the growth stages in the different durations (2, 4 and 6 h). Furthermore, additional deposition experiments are conducted on these specimens at different substrate temperatures (650, 800 and 950 °C), and WC−12%Co substrates with different Co-removal depths at a definite substrate temperature of 950 °C, adopting different growth durations in order to obtain diamond films of similar thickness, which are used for evaluating the film−substrate adhesion.

The surface and cross-sectional morphologies of the specimens were observed by FESEM. The corresponding surface chemical compositions were evaluated by the XPS (Axis Ultra DLD, Kratos, Japan) surface analysis, and the Co contents on the deposited surfaces were detected by either the EDX or the XPS analyses. Raman spectra of typical specimens were obtained by the Confocal Raman Microscopy (Senterra R200−L, Bruker, Germany) using a laser with a visible excitation wavelength of 532 nm. The adhesion of the diamond film is approximately evaluated by a Rockwell hardness tester (HR−150A, Beijing Shidai, China), adopting a definite load of 980 N. Moreover, The Stylus Profiler (*Dektak 6M*, Veeco, USA) was used for measuring the surface roughness (R_a) values of some samples.

3 Results and discussion

3.1 Effects of pretreatment parameters on *D* of WC−Co substrates with different Co contents

Surface morphologies of WC−Co specimens with different Co contents after the Murakami pretreatment (x=100 mL, T_M=15 min) and after the whole pretreatment (x=100 mL, T_M=15 min, y=0 mL, T_{ac}=30 s, including the Murakami-acid and the subsequent abrading) are all shown in Fig. 3, along with elementary compositions. As-measured surface roughness (R_a) values of corresponding specimens are plotted in Fig. 4, and noteworthy is that each value is obtained by averaging five values at different positions, and bars for columns indicate errors. It is clear that for the three specimens, variations of the Co content on the surface and the R_a value along with the pretreatment process are almost the same: 1) The Murakami pretreatment can increase either the Co content or the R_a value, because

Table 3 Experimental parameters used in nucleation, growth or heating experiments

Procedure	Flux of hydrogen/ (mL·min^{-1})	Flux of acetone/ (mL·min^{-1})	Pressure/ Pa	Substrate temperature/ °C	Filament length/ mm	Filament diameter/ mm	Filament separation/ mm	Filament height/ mm	Duration/ min
Nucleation	800	20	1600	650, 800, 950					20
Growth	800	20	3300	900	110	0.6	32	−5	120, 240, 360
Heating	800	0	1600	650, 800, 950					20

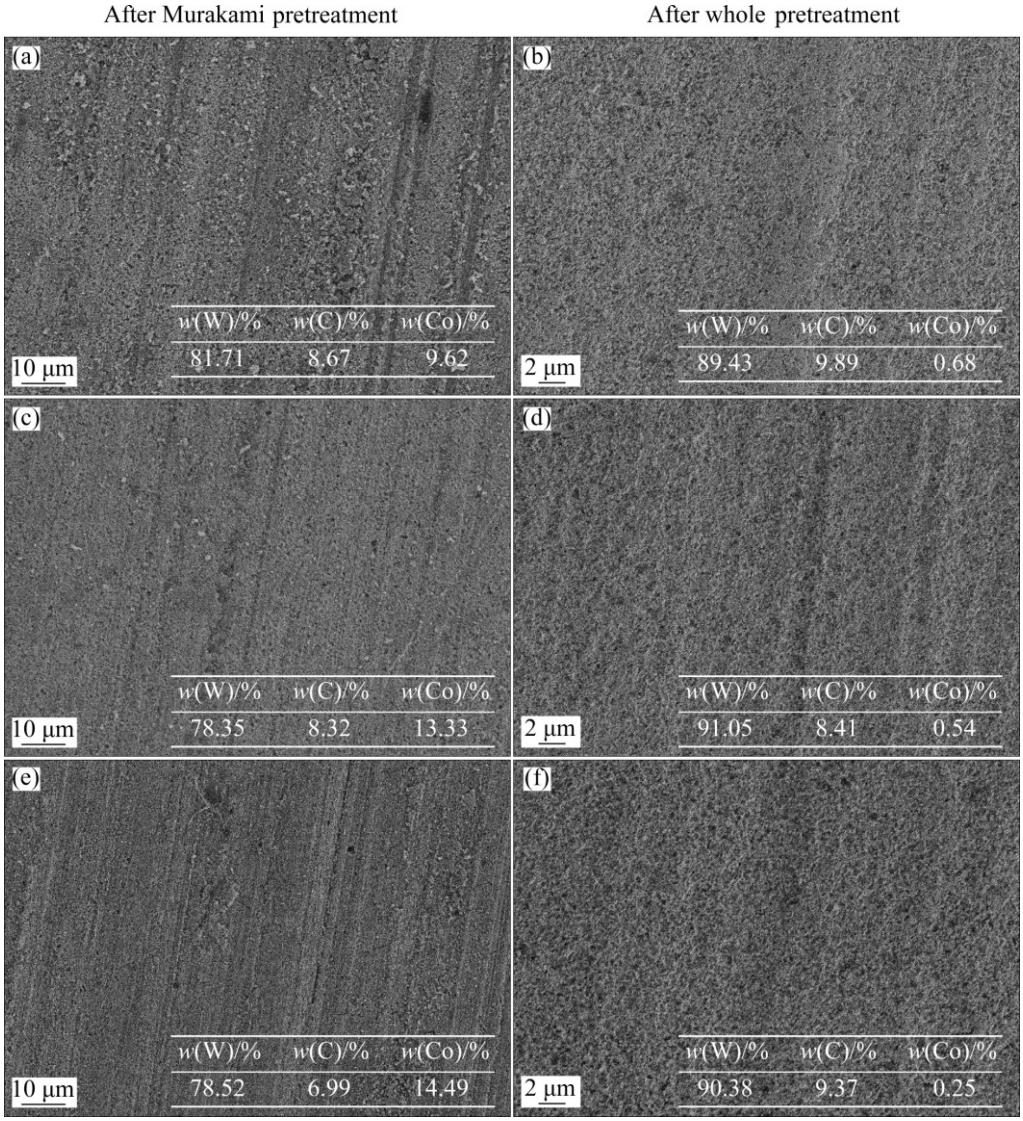

Fig. 3 Surface morphologies of WC−Co specimens with 6% Co (a, b), 10% Co (c, d) and 12% Co (e, f) after Murakami pretreatment (x=100 mL, T_M=15 min) (a, c, e) and after whole pretreatment (x=100 mL, T_M=15 min, y=0 mL, T_{ac}=30 s, including Murakami-acid pretreatment and subsequent abrading pretreatment) (b, d, f) together with elementary compositions marked in inserted tables

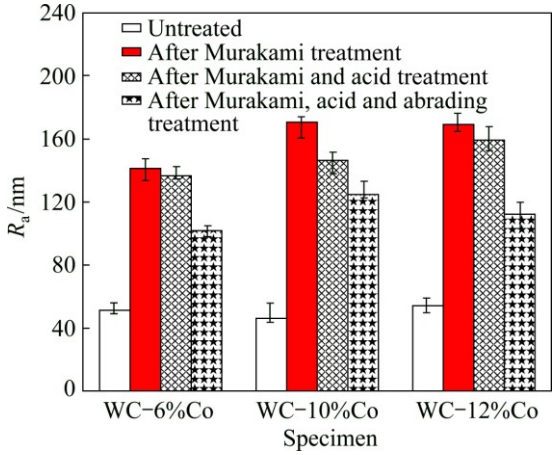

Fig. 4 Surface roughness (R_a) values of WC−Co specimens with different original Co contents at different stages of pretreatment

the Murakami solution can selectively etch part of the W on or close to the surface [36]; 2) Acid and abrading can gradually decrease the R_a value of the surface, owing to the selective removal of the Co in the acid pretreatment, and the probable simultaneous removal of the WC and residual Co in the loose surface layer caused by the abrading. After the whole pretreatment, Co contents on surfaces of three substrates all reduce to below 0.7%, indicating that such the pretreatment can sufficiently remove the Co on the surface, regardless of the original Co content.

Cross-sectional morphologies of first three specimens in orthogonal pretreatment tests (No. 1−3 in Table 3) are shown in Fig. 5, along with elementary compositions at different positions and variations of Co contents along the depth direction (the position of the

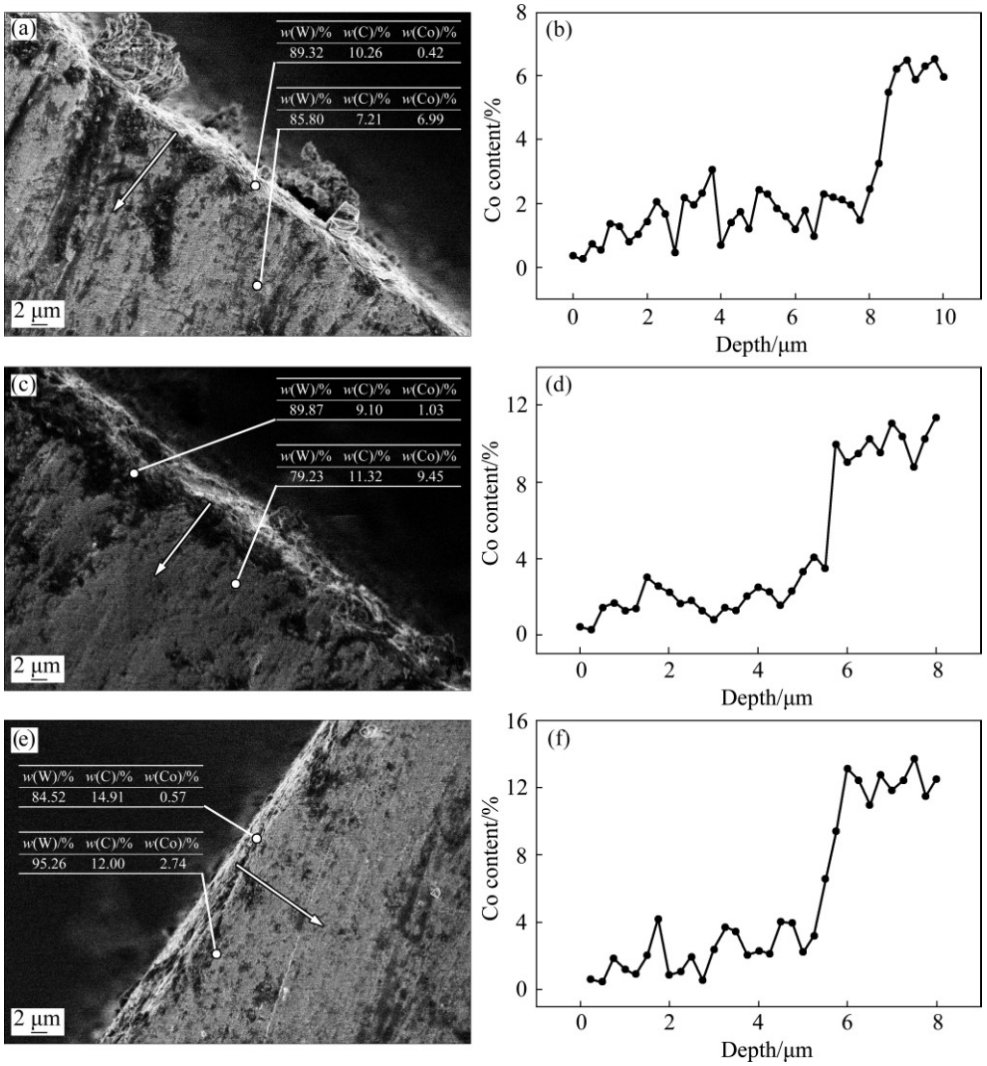

Fig. 5 Cross-sectional morphologies (a, c, e) and variations of Co content along depth direction (b, d, f) of typical specimens of Case 1 (a, b), Case 2 (c, d) and Case 3 (e, f) in Table 2, along with elementary compositions at different positions as listed in inserted tables and variations of Co content along depth direction (position of arrow plotted in FESEM micrograph)

arrow plotted in the FESEM micrograph), which are all detected by the integrated EDX in the FESEM. It is clear that there are different D for different specimens. Besides, experimental results (D) for all the cases in orthogonal pretreatment experiments are stated in Table 2, including results of the range analysis. Herein, each of the D value is obtained by averaging five values at different positions. From the range analysis, following conclusions are drawn.

1) The volume of the water in the acid solution y has the most significant effect on the D. The increment of y, meaning the more dilution and the rapid reduction of the chemical reactivity of the acid solution, will cause the apparent reduction of the D.

2) The time of the acid pretreatment T_{ac} has the second most significant effect on the D, because this factor directly controls the progressive depth of the reaction.

3) With increasing the Co content in the substrate, the D slightly decreases, for more Co elements require more reactions to be removed.

4) The Murakami pretreatment acts as a subsidiary role in affecting the D, especially the volume of the water in the Murakami solution y, which performs slight and irregular influence on the D in the selected range, because such dilution in a certain extent may not apparently affect the reactivity of the Murakami solution. While the time of the Murakami pretreatment T_M still has minor and regular effects, concretely, the increment of the T_M can slightly increase D, probably because the long-time and sufficient Murakami pretreatment can remove WC grains more effectively and more-exposed Co elements are easier to be removed by the subsequent acid solution.

As discussed above, because the effect of the y on the D is too significant but it is very difficult to control the D by adjusting the y, in the following experiments, the T_{ac}, which has an appropriate effect on the D, is

selected as the only variable for preparing required specimens, including WC−6%/10%/12%Co substrates with almost the same D (8−9 μm), and WC−12%Co substrates with the different D.

3.2 Results of nucleation tests on pretreated or untreated WC−Co substrates

On the basis of above researches, the pretreatment parameters for preparing the WC−6%/10%/12%Co substrates with similar D are finally determined as: x=100 mL, T_M=15 min, y=0 mL, T_{ac}(WC−6%Co)=30 s, T_{ac}(WC−10%Co)=35 s, T_{ac}(WC−12%Co)=40 s. As proved by the corresponding EDX detection results, D values for all the specimens are limited in the range of 8−9 μm, and the Co contents on the surfaces are respectively 0.68%, 0.42% and 0.61% for the specimens with original Co contents of 6%, 10% and 12%.

Surface morphologies of typical specimens after the nucleation experiments are shown in Fig. 6, based on which the nucleation density (ND) and nuclei size (NS) are calculated. Herein, the ND is evaluated in term of the number of diamond crystals on a unit square millimeter, and the NS is defined as the mean diameter of diamond nuclei [37]. Each of the ND of NS value is also obtained by averaging corresponding values at five different positions. As-calculated ND and NS values for all the specimens after the nucleation experiments are plotted in Figs. 7(a) and (b), firstly indicating that both the indexes for all the specimens approximately increase with the substrate temperature, because substrate temperatures in the present study (650−900 °C) are appropriate for synthesizing the HFCVD diamonds, and the increase of the substrate temperature can provide more energy for promoting the diamond nucleation and growth [38]. However, when increasing the substrate temperature from 800 °C to 950 °C, the changes of the ND values for the pretreated WC−6%/10%Co specimens are minuscule, for after the 20 min nucleation at the substrate temperature of 800 °C, the diamond nuclei have almost totally covered the substrate surfaces.

From each of the curve, it can be demonstrated that under most of the conditions (different substrate temperatures, treated or untreated specimens), ND and NS values will both become smaller for the specimen with relatively high original Co content. For the untreated specimens, such change is easily understood, because the higher Co content on the substrate surface will significantly repress the diamond nucleation. For the pretreated specimens with almost the same D and Co-free surface, such change is speculated to be caused by the subsequent diffusion of the Co element from the inside to the surface of the substrate under high-

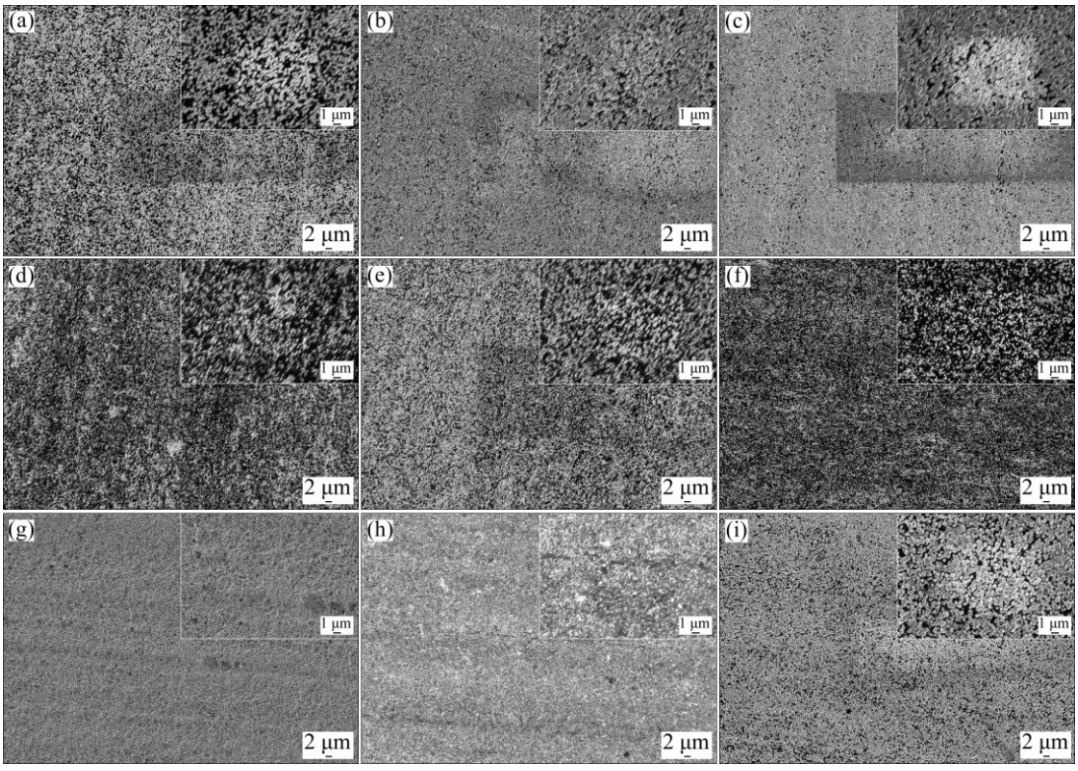

Fig. 6 Surface morphologies of typical specimens after nucleation experiments: (a) Pretreated WC−6%Co after 650 °C nucleation; (b) Pretreated WC−6%Co after 800 °C nucleation; (c) Pretreated WC−6%Co after 950 °C nucleation; (d) Pretreated WC−10%Co after 650 °C nucleation; (e) Pretreated WC−10%Co after 800 °C nucleation; (f) Pretreated WC−12%Co after 650 °C nucleation; (g) Untreated WC−6%Co after 650 °C nucleation; (h) Untreated WC−6%Co after 800 °C nucleation; (i) Untreated WC−6%Co after 950 °C nucleation

temperature nucleation conditions, which will be discussed later. Also as a result of the significant difference between the Co contents on the substrate surfaces, compared with the diamond nucleations on the pretreated surfaces, those on the untreated surfaces are retarded. When the substrate temperature is as low as 650 °C, no nucleation sign appears on the surfaces of all the untreated specimens. When the substrate temperature is 800 °C, the NS values for all the untreated specimens are below 0.1 μm, which are difficult to be distinguished and thus uniformly defined as 100 nm in Fig. 7(b). However, at the substrate temperature of 950 °C, the difference between the diamond nucleations on the surfaces of pretreated and untreated specimens are not as significant as that at the substrate temperatures of 650 and 800 °C, probably due to the etching of the surface Co element caused by the high temperature [34], which will be discussed later based on the XPS and EDX analyses.

XPS spectra for the selected typical specimens are plotted in Fig. 8(a), presenting expected peaks related to the C, W and Co elements, which are all further detected

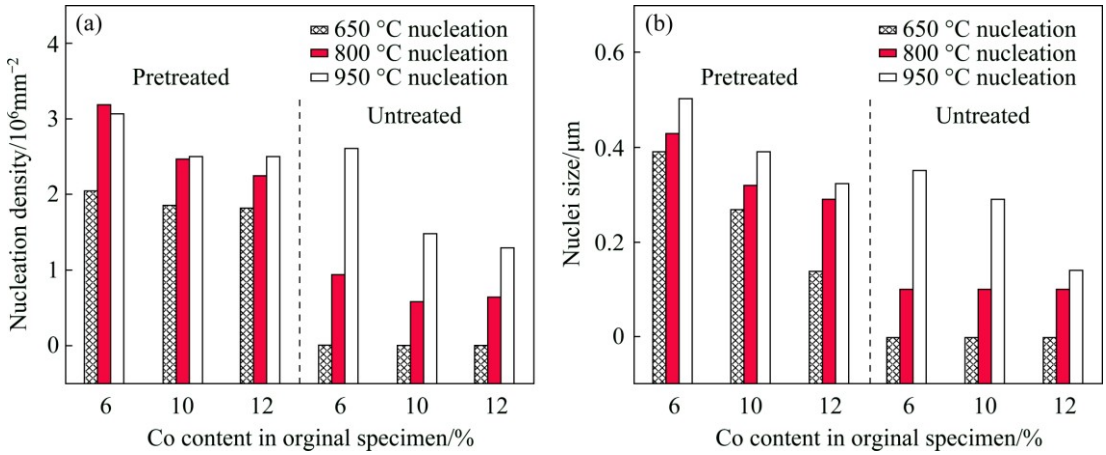

Fig. 7 Nucleation density (a) and nuclei size (b) of pretreated or untreated WC−6%/10%/12%Co specimens after 20 min nucleation experiments at different substrate temperatures

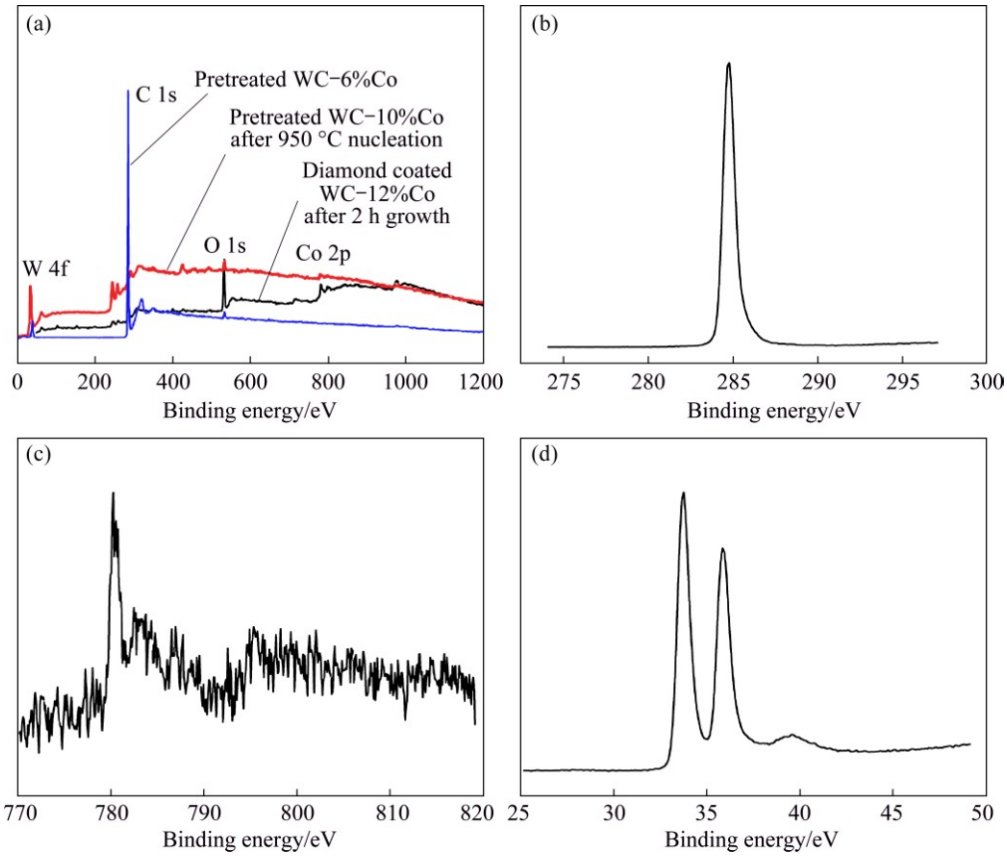

Fig. 8 Whole XPS spectra of selected typical specimens (a), and high-resolution XPS spectra respectively related to C 1s (b), Co 2p (c) and W 4f (d) elements for pretreated WC−10%Co specimen after 950 °C nucleation

by high-resolution and short-range XPS scanning, as exemplified in Fig. 8(b)−(d). It is found that the XPS spectrum related to the Co mainly exhibits two contributions, including the peak around 779.2 eV ascribed to the cobalt oxide and the peak around 793.7 eV that should be assigned to elemental Co 2p. Apparently, for the typical pretreated WC−6%Co specimen, the Co 2p peak can hardly be noticed in the corresponding XPS spectrum. The C 1s peak around 285 eV can be attributed to the existence of the diamond phase synthesized in the present study, and the peaks located in the range of 30−34 eV correspond to W 4f. For the typical diamond coated WC−12%Co specimen fabricated in a growth duration of 2 h, there have been no clear W 4f peaks, mainly owing to the complete coverage of the diamond film on the substrate. In the following discussions, the Co/W mole ratio is approximately calculated based on intensities of the Co 2p and the W 4f peaks, which is adopted as an important criterion for evaluating the Co evolution [33].

For the different specimens after 20 min nucleation at different substrate temperatures (650, 800, 950 °C), the Co/W mole ratios on substrate surfaces calculated based on the XPS spectra and the Co contents on substrate surfaces measured by the EDX are respectively plotted in Figs. 9(a) and (b), presenting satisfied consistence. It is proved that for all the treated surfaces with rather low Co contents, there are no clear changes in such the Co contents after nucleation at the substrate temperature of 650 °C. Nevertheless, the substrate temperatures as high as 800 and 950 °C can cause considerable increment of the Co content, and the higher the substrate temperature, the larger such the increment. Moreover, although the three different treated specimens have similar Co contents (0.42%−0.68%) on the surfaces, after 800 and 950 °C nucleation, apparent difference appears, that is, the higher the original Co content in the WC−Co specimen, the higher the Co content on the substrate surface after the nucleation experiments. It is believed that such difference mainly results from the different Co content gradients from the surface to the inside of the pretreated specimens (0.7%/μm for WC−6%Co, 1.2%/μm for WC−10%Co, 1.4%/μm for WC−12%Co). Based on the Fick's first law, the larger the concentration difference (the Co content gradient), the quicker the Co diffusion. It would stand to reason that such Co diffusion plays a dominant role in affecting the ND and NS on the surfaces of the pretreated specimens, well explaining the differences as discussed above.

For all the three untreated specimens, the nucleation experiments at the substrate temperatures of 650 and 800 °C have no clear influences on the Co contents on the substrate surfaces, which are originally as high as

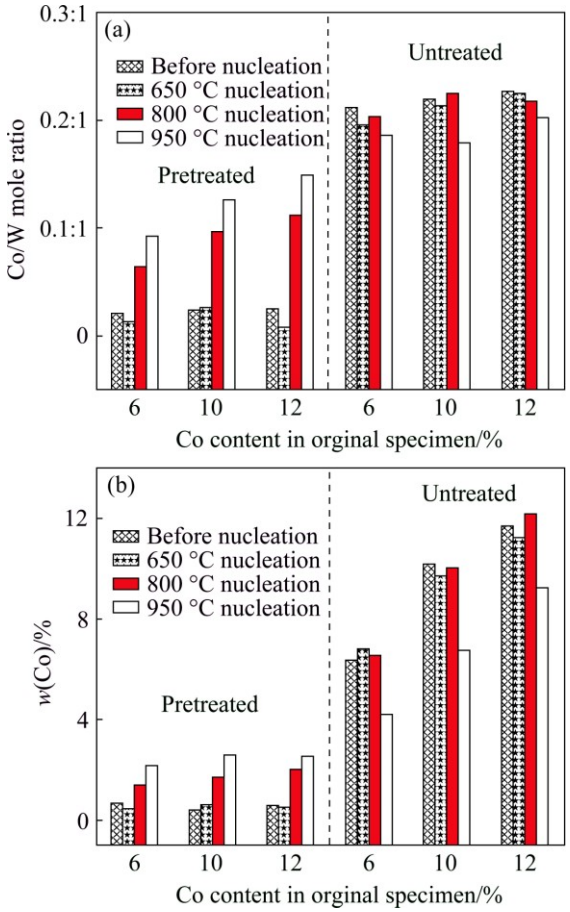

Fig. 9 Co/W mole ratio on substrate surface calculated based on XPS spectra (a) and Co content on substrate surface measured by EDX (b) for either pretreated or untreated WC−6%/10%/12%Co specimens after 20 min nucleation at different substrate temperatures

6%−12%. Interestingly, the even higher substrate temperature (950 °C) will significantly reduce the Co content on the surface, which should be attributed to the function analogous to the high-temperature etching pretreatment. Consequently, for a certain specimen, the difference between the Co contents on the surfaces of the untreated and pretreated specimens at the substrate temperature of 950 °C is not as large as those at the substrate temperatures of 650 and 800 °C. Such analysis can explain why at the substrate temperature of 950 °C, the difference between the diamond nucleations on pretreated and untreated specimens is not as significant as that at the substrate temperatures of 650 and 800 °C.

Raman spectra of some typical specimens are illustrated in Fig. 10(a), all showing similar shapes. For any spectrum, the peak around 1332.4 cm^{-1} is the characteristic peak of the sp^3 diamond, the disordered carbon band (D band, around 1350 cm^{-1}) and the graphitic band (G band, around 1580 cm^{-1}) represent the contributions from some sp^2 components, and the two

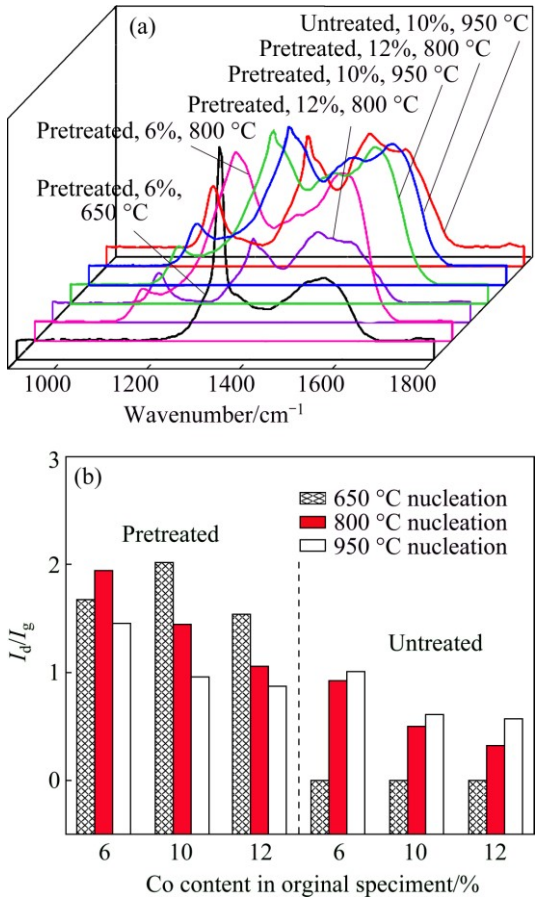

Fig. 10 Raman spectra of typical specimens after nucleation experiments (a) and as-calculated I_d/I_g intensity ratios for pretreated and untreated specimens after nucleation experiments (b)

peaks around 1150 cm^{-1} and 1480 cm^{-1} are both assigned to the transpolyacetylene [39]. The integral intensity ratio of the diamond peak to the graphitic peak (I_d/I_g) is defined for evaluating the degree of graphitization, as plotted in Fig. 10(b). Combining the analyses of the preceding contexts, it is firstly clarified that as compared with the pretreated specimens, the untreated ones present apparently lower I_d/I_g ratios after the nucleation experiments at the different substrate temperatures, indicating that more graphites exist on the surfaces, which are mainly attributed to the effect of the more Co element on the surface. Owing to the similar reason, at relatively high substrate temperatures (800 and 950 °C), the I_d/I_g ratio for any of the untreated or the pretreated specimen significantly decreases with increasing the Co content in the original specimen. Moreover, for the pretreated specimens, such I_d/I_g ratio reduces with increasing the substrate temperature, due to the Co diffusion from the inside to the surface of the substrate in the nucleation experiment. On the contrary, such ratio slightly rises with increasing the substrate temperature for the untreated specimens, which is also attributed to the function analogous to the high-temperature etching.

3.3 Co evolution in pretreated and untreated specimens in heating experiments

In the nucleation experiments, the function provided by the substrate temperature as high as 950 °C, which is analogous to the high-temperature etching pretreatment, might be more or less affected by the nucleation process or the diamond nuclei, so the heating experiments in the same duration (20 min) at the corresponding substrate temperatures (650, 800 and 950 °C) are also accomplished, adopting the WC−12%Co substrate as the example. After the heating experiments, the Co/W mole ratio and the Co content on the substrate surface are both plotted in Fig. 11, including corresponding results in the nucleation experiments, which are used as comparison.

For the pretreated specimens, the Co/W mole ratios on substrate surfaces after heating are higher than those after nucleation. It is known that the detection depth of the XPS is only several nanometers, so as-measured Co/W mole ratio on the nucleated surface is the Co/W mole ratio on the real surface of the specimen but not exactly on the substrate surface. As a result, it is recognized that such difference is caused by as-deposited diamond nuclei covering part of or even the whole substrate surface, which may work in two ways. Firstly, the diamond nuclei can hinder the Co diffusion from the diamond-substrate interface (the actual substrate surface) to the real surface of the specimen. Secondly, as-deposited diamond nuclei can also cause a slight temperature difference from the real specimen surface to the diamond-substrate interface, so in the nucleation experiment, the actual substrate temperature directly affecting the Co diffusion from the inside to the surface of the substrate is slightly lower than that in the heating experiment.

For the untreated specimen, at relatively high substrate temperatures of 800 and 950 °C, the Co/W mole ratio on the substrate surface after heating is lower than that after the nucleation, and the higher the temperature, the larger the difference. It is supposed that such difference is also caused by the existence/inexistence of diamond nuclei covering part or even the whole substrate surface. Herein, the bare substrate surfaces in the heating experiments are much easier to be directly affected at the high temperatures (800 and 950 °C), and the Co element on the surfaces can diffuse from the substrate surface to the atmosphere much more efficiently, especially at the substrate temperature as high as 950 °C, which is almost the same as the condition of the high-temperature etching pretreatment.

It should be noted that in above studies conducted on the pretreated specimens, such Co diffusion from the substrate surface to the atmosphere cannot be directly

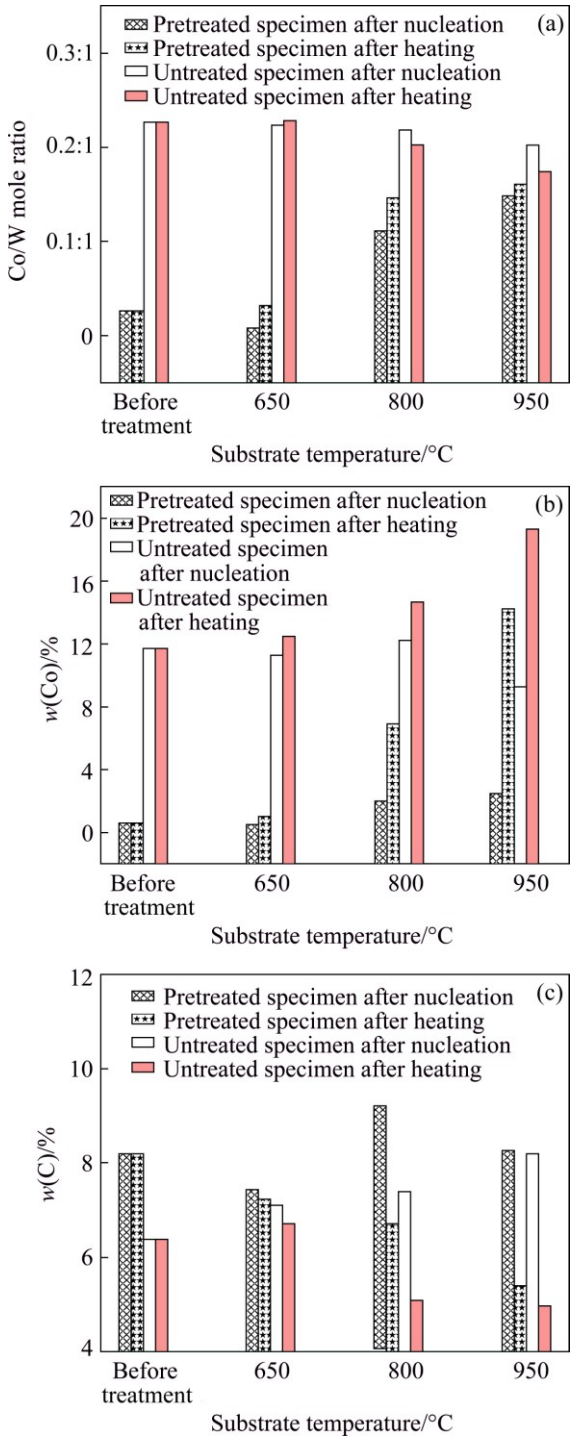

Fig. 11 Co/W mole ratio on substrate surface (a), Co content (b) and C content (c) on substrate surface of pretreated and untreated WC−12%Co specimens after heating at different substrate temperatures including corresponding results after nucleation experiments as comparison

proved. However, there is still natural Co content gradient from the substrate surface to the atmosphere, which has no theoretical difference as compared with that for the untreated specimens, so the Co diffusion from the substrate surface to the atmosphere is still supposed to exist when the substrate temperature is high enough, which along with the Co diffusion from the inside to the surface of the substrate constitute a dynamic balance system. As demonstrated by above comparisons, the Co contents on the surface of the pretreated specimens after heating are higher than those after nucleation, demonstrating that the inhibition effect of as-nucleated diamonds on the Co diffusion from the substrate surface to the atmosphere has not been reflected, in other words, in such dynamic balance system, the Co diffusion from the inside to the surface of the substrate still dominates.

As presented in Fig. 11(b), the Co contents on the substrate surface measured by the EDX show totally different variation trend, i.e., clear increment of the relative Co contents on the substrate surface after heating, especially at the relatively high substrate temperatures (800 and 950 °C), because under the heating conditions without carbon source, H_2 can decarbonize WC, and thus induce the significant increment of the relative Co content, which are further proved by the approximate C content plotted in Fig. 11(c). Consequently, it can be concluded that after heating the relative Co content cannot be directly used as the criterion for evaluating the Co evolution.

3.4 Results of experiments conducted on pretreated specimens with different *D*

Based on above discussion, it is found that the higher the substrate temperature or the Co content in the original specimen, the more dramatic the Co evolution for the pretreated substrate after either nucleation or heating. Therefore, in the present study, the WC−12%Co specimens are selected as the substrates, on which the two-step Murakami-acid pretreatments at different T_{ac} (20, 30, 40, 60 and 80 s) are conducted, and thus the pretreated WC−12%Co specimens with different D (5.2, 7.0, 8.4, 9.4 and 10.2 μm) are successfully prepared. Besides, the highest and typical substrate temperature (950 °C) in the foregoing experiments is determined as the substrate temperature in the present nucleation and heating experiments conducted on as-prepared WC−12%Co specimens with different D, and the duration is defined as 20 min. Since it is not appropriate to adopt the relative Co content measured by the EDX as the criterion to evaluate the Co evolution in the heating experiments. In the present study, only the Co/W mole ratios on the substrate surfaces are calculated based on the XPS analyses, as plotted in Fig. 12.

Firstly, it is found that all the specimens present rather low Co/W mole ratios on the pretreated surfaces before nucleation or heating, regardless of the T_{ac}, indicating that selected pretreatment procedures can fully ensure the removal efficiency of Co on the surface.

Secondly, the difference between the Co/W mole ratios after nucleation and heating is always consistent with that in the experiments as discussed above, i.e., for any of the specimens, the Co/W mole ratio after heating is higher than that after nucleation. Thirdly, with increasing D from 5.2 to 8.4 μm, the Co/W mole ratio after either nucleation or heating clearly decreases, but the further increment of D has minuscule influence on the Co/W mole ratio. It is easily understood that in the range of 5.2−8.4 μm, the thicker the corrosion layer, the smaller the Co content gradient in such layer, and the slower the Co diffusion from the inside to the surface in any of the experiments. Moreover, because the influence of D on the Co/W mole ratio gradually weakens when increasing the D to some levels, and it can be additionally found from the preparation of the WC−12%Co specimens with different D values that when the D reaches 8.4 μm, even larger D requires much more pretreatment time. Moreover, it is also known that in many application cases [40], the larger D often means the more significant toughness reduction of as-fabricated diamond coated components. Consequently, it is supposed that in the present work, a T_{ac} of 40 s corresponding to a D value of 8−9 μm should be an optimal solution for pretreating the Co-rich WC−Co substrate.

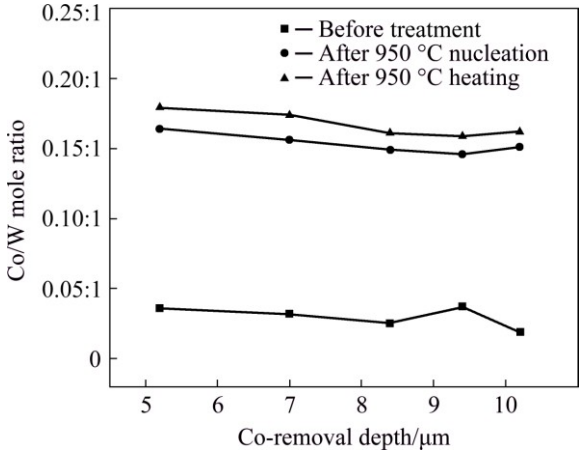

Fig. 12 Co/W mole ratio on substrate surface of pretreated WC−12%Co specimens with different Co-removal depth (D) after nucleation and heating in same duration of 20 min at substrate temperature of 950 °C

3.5 Influence of film thickness on Co evolution

Deposition experiments are conducted on pretreated WC−Co substrates with the different original Co contents but the same D, at the same substrate temperature of 900 °C in nucleation duration of 20 min, but the different growth durations (2, 4 and 6 h) corresponding to the different film thicknesses. Due to the total coverage of the diamond film on the substrate surface, the W element can hardly be detected by the XPS, as shown in Fig. 8, as a result, in the present deposition experiments, only the Co content on the film surface measured by the EDX is adopted as the criterion for evaluating the Co evolution, as shown in Fig. 13. Firstly, it can also be found that at the substrate temperature of 900 °C, the Co contents on the substrate surfaces apparently increase after 20 min nucleation, in conformity with above descriptions. For a relatively short growth duration of 2 h, the Co elements can still be detected on the surfaces of as-deposited diamond films, for part of the Co elements can continue to diffuse from the film−substrate interface to the surface of as-deposited diamond film along the grain boundaries [41]. Nevertheless, with the extension of the growth duration and the increase of the film thickness, the Co contents on the film surfaces decrease to rather low levels and even zero, probably owing to the barrier action of the well-grown diamond crystals. In addition, approximately, the higher the original Co content in the substrate, the higher the Co content after the pretreatment, the higher the Co content after the high-temperature diamond nucleation, the higher the Co content after the short-duration film growth, and the longer duration required for eliminating the Co diffusion from the film−substrate interface to the film surface, which are all caused by the larger Co content gradient in the pretreated substrate as proved before. Nevertheless, because it is the Co element close to the film−substrate interface that plays the most important role in the film−substrate adhesion, such the elimination of the Co diffusion after relatively long growth duration does not seem to make a lot of sense.

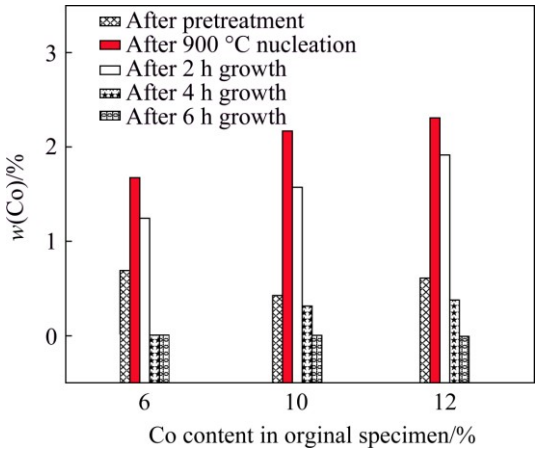

Fig. 13 Co content on surfaces of diamond films owning different thicknesses deposited on pretreated WC−6%/10%/12%Co specimens with same D, at same substrate temperature of 900 °C in nucleation duration of 20 min, including Co content on pretreated and as-nucleated surfaces

Cross-sectional morphologies of the diamond coated specimens are presented in Fig. 14, including the

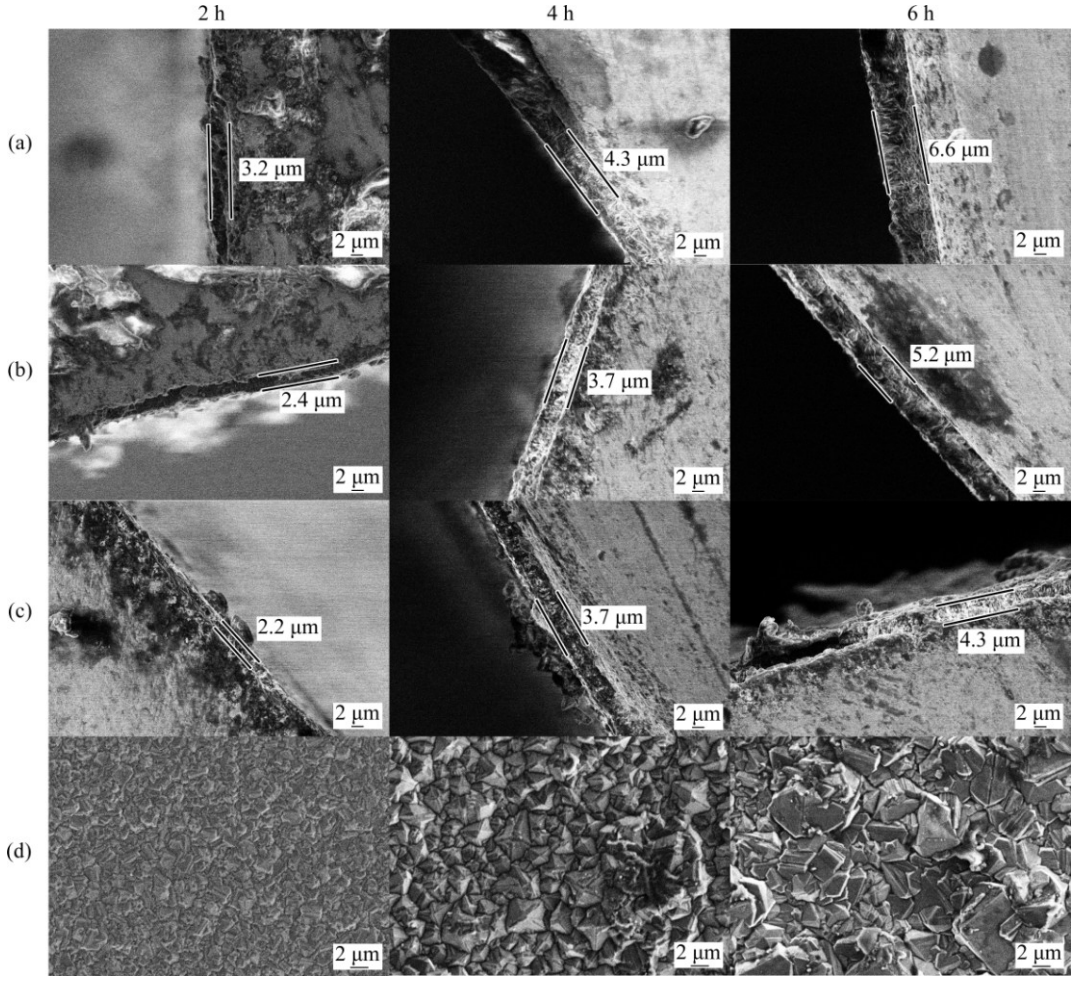

Fig. 14 Cross-sectional morphologies and as-measured thicknesses of diamond films synthesized for different growth time on pretreated WC−6%Co (a), WC−10%Co (b) and WC−12%Co (c) substrates, as well as typical surface morphologies of diamond films deposited on WC−12%Co substrate (d)

typical surface morphologies of as-deposited diamond films on WC−12%Co substrates. It can be visually indicated that the diamond film shows higher growth rate on the pretreated WC−Co specimen with lower original Co content, because the more Co element diffusing from the inside to the surface of the substrate and even to the film surface can inhibit not only the nucleation but also the growth of the diamond along the thickness direction. Moreover, it is supposed that for the pretreated WC−Co substrate with relatively high original Co content, besides the high Co content gradient in the substrate, such reduction of the growth rate can also prolong the required duration for eliminating the further Co diffusion from the film−substrate interface to the film surface.

In addition, the Raman spectra of several typical diamond coated specimens are plotted in Fig. 15(a). It is acknowledged that during the diamond nucleation and growth processes, the residual Co element on as-pretreated substrate surface, along with the Co diffusion from the inside to the surface of the substrate and even to the surface of as-grown diamond film will induce significant graphitization, and thus deteriorate the diamond purity of as-deposited diamond film, generally manifesting as the reduction of the intensity of the sp^3 diamond Raman peak, the broadening of such diamond peak, and the appearance and enhancement of the Raman peaks related to the graphite or some other non-diamond phases.

As presented in Fig. 15(a), it is firstly demonstrated that the typical micro-crystalline diamond (MCD) films growing on the three different substrates for 6 h all present perfect Raman line shapes similar to the natural diamond, because well-grown diamond crystals growing for 6 h can provide sufficient barriers for restraining the Co diffusing to the positions at or close to the film surface, and the MCD film is supposed to have extremely high intrinsic diamond purity without regard to the pollution of the growth environment caused by the Co element or some other factors. On the contrary, clear graphite peak appears in the Raman spectrum of the MCD film deposited on the WC−6%Co substrate in a growth duration of only 2 h, which is attributed to the

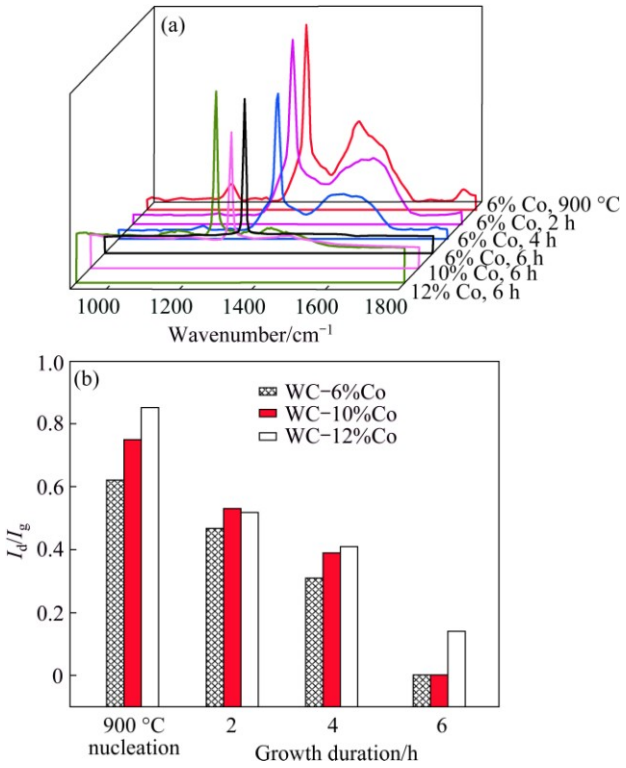

Fig. 15 Raman spectra of several typical diamond coated specimens (a) and as-calculated I_g/I_d intensity ratios for pretreated specimens after 900 °C nucleation for different growth durations

effect of the relatively high Co content close to the growth face. Corresponding to the specimens in Fig. 13, the I_g/I_d values are all illustrated in Fig. 15(b), approximately demonstrating the relationship between the Co content and the diamond purity, i.e., with the increase of the film thickness and the reduction of the Co content on the surface of as-deposited diamond film, the I_g/I_d value decreases; on the pretreated substrate with high original Co content, as-deposited MCD film performs high I_g/I_d value, which is especially apparent when the film thickness is insufficient for totally restraining the Co diffusion. It should be emphasized that in Fig. 10 I_d values are zero for some specimens, while in Fig. 15, I_g values are zero for some specimens, considering the convenience of the calculation, the I_d/I_g is adopted as the criterion in Fig. 10, but the I_g/I_d value is adopted in Fig. 15.

3.6 Adhesion of as-deposited diamond films under typical conditions

It is believed that the film−substrate adhesion is technologically the most important issue for the application of the CVD diamond film, which is closely associated with the Co content and related diamond quality at the interface. Moreover, it is known that the adhesion approximately evaluated by the indentation test is well associated with the film thickness, and the thickness is influenced by either the original Co content or the substrate temperature, so based on Fig. 14 and some other corresponding tests, under the different conditions (certain substrate temperature and original Co content), growth durations are elaborately determined for obtaining similar film thicknesses (6.8−7.4 μm), as listed in Table 4. As exemplified in Fig. 16, under the definite indentation load of 980 N, as-synthesized diamond coated specimens of similar film thicknesses all present clear film fracture and even extended cracks, but different fracture areas. As a result, diameters of fracture areas or crack extension lengths, which are uniformly defined as A_f, are adopted to approximately evaluate their adhesion. Also as listed in Table 4, each the A_f value is obtained by calculating as-measured values on five different specimens. It is noted that for as-deposited diamond films of similar thickness, the film−substrate adhesion is mainly influenced by interface characteristics, such as the Co content at or close to the interface (Fig. 9) and the subsequent diamond quality at the nucleation or initial growth stages (Fig. 10). More non-diamond phases at the interface will contribute to the in-site residual stress and deteriorate the film−substrate adhesion. As a result, it is found that with increasing the substrate temperature, the film−substrate adhesion will slightly reduce, owing to the reduced I_d/I_g (Fig. 10) caused by the more significant diffusion of the Co element from the inside of the substrate to the interface (Fig. 9). Similarly, it is also easily understood that for the WC−Co substrate with high original Co content, as-deposited diamond film presents relatively poor adhesion.

Table 4 Fracture areas for diamond films deposited on substrates with different original Co contents at different substrate temperatures

Original Co content/ %	Substrate temperature/ °C	Growth duration/ h	Actual film thickness/ μm	A_f/ mm
6	650	11	6.9	0.52
6	800	7	7.3	0.55
6	950	6	7.1	0.67
10	650	14	7.0	0.57
10	800	9	7.1	0.69
10	950	7.5	6.9	0.95
12	650	16	6.9	0.58
12	800	11	7.2	0.81
12	950	9.5	7.1	1.01

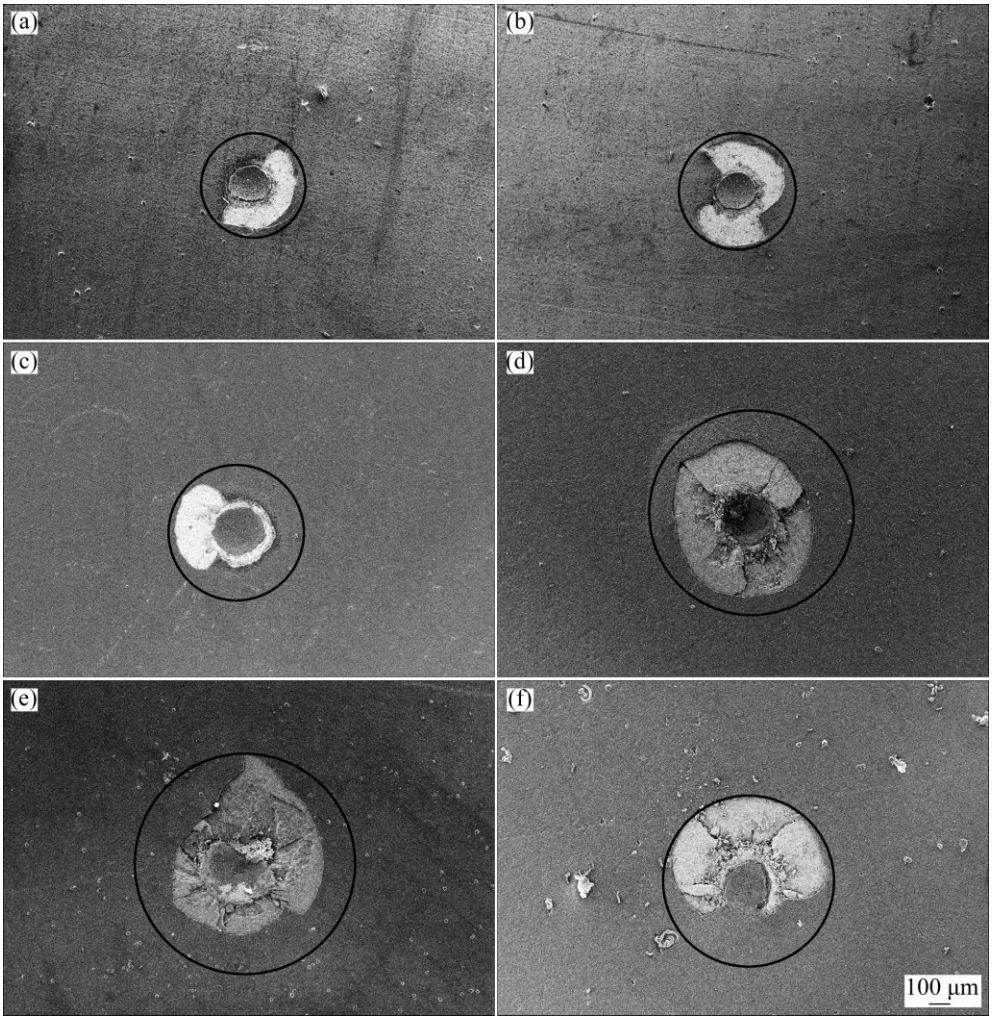

Fig. 16 Typical indentation morphologies of diamond films with similar thickness (6.8−7.4 μm) deposited on different substrates at different substrate temperatures: (a) WC−6%Co, *D*=8−9 μm, 650 °C; (b) WC−6%Co, *D*=8−9 μm, 800 °C; (c) WC−6%Co, *D*=8−9 μm, 950 °C; (d) WC−10%Co, *D*=8−9 μm, 950 °C; (e) WC−12%Co, *D*=8−9 μm, 950 °C; (f) WC−12%Co, *D*=10.2 μm, 950 °C

Experimental results on WC−12%Co substrates with different *D* are shown in Table 5, corresponding to Fig. 12, proving that with increasing *D*, because the diffusion of the Co from the inside of the substrate to the interface can be significantly suppressed, as-deposited diamond film presents improved adhesion, which can even deposit on the WC−6%Co substrate, as demonstrated by Figs. 16(c) and (f). As a result, it is supposed as a simple method to increase the *D* for enhancing the adhesion of the diamond film deposited on the Co-rich WC−Co substrate, regardless of the toughness of as-fabricated diamond coated WC−Co components.

Table 5 Fracture areas under indentation load of 980 N for diamond films deposited on WC−12%Co substrates with different Co-removal depths *D*

D/μm	Growth duration/h	Actual film thickness/μm	A_f/mm
5.2	11.0	7.1	1.17
7.0	10.5	7.3	1.14
8.4	9.5	7.1	1.01
9.4	9.0	7.2	0.88
10.2	7.5	6.9	0.73

3.7 Co evolution mechanisms

On the basis of above results and discussion, the evolution mechanisms of the Co element in WC−Co substrates during the whole manufacturing processes of diamond coated components, including the pretreatment, nucleation and film growth, together with the similar mechanism in a heating process in the hydrogen atmosphere, and the evolution mechanisms of the Co elements in the untreated WC−Co substrates during the same nucleation and heating processes, are summarized, as demonstrated in Fig. 17.

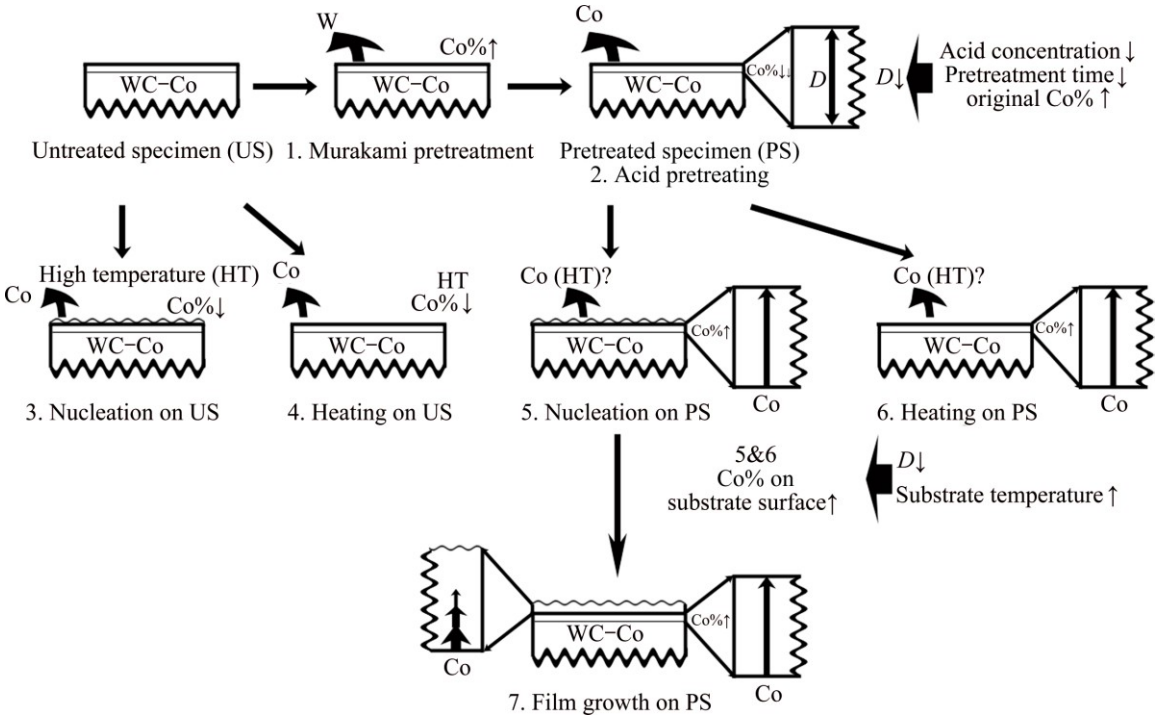

Fig. 17 Evolution mechanisms of Co element in WC−Co substrates during all experimental processes

1) The Murakami pretreatment will etch part of the W element, and thus indirectly increase the Co content on or close to the substrate surface.

2) The acid pretreatment can significantly reduce the Co content on or close to the substrate surface as expected. The Co-removal depth is closely associated with the acid concentration, pretreatment time and the original Co content in the substrate, which is easily understood.

3) During the nucleation experiments conducted on the untreated specimens, at a substrate temperature as high as 950 °C, the Co content slightly reduces, due to the function analogous to the high-temperature etching pretreatment, i.e., the diffusion of the Co element from the substrate to the atmosphere at high temperatures.

4) During the heating experiments at the high substrate temperature of 950 °C which are also conducted on the untreated specimens, because there are no as-nucleated diamonds that will hinder the diffusion of the Co element from the substrate to the atmosphere, the reduction of the Co content is more apparent.

5) During the nucleation experiments conducted on the pretreated specimens, the Co content on the substrate surface presents a significant increment, because the high temperature can promote the Co element inside the substrate diffusing to the surface. The higher the substrate temperature, or the shorter the D, the more the increment of the Co content on the substrate surface.

6) During the heating experiments conducted on the pretreated specimens, the rising of the Co content is more clear than that during the nucleation experiments. As the question marks in either the nucleation or the heating experiments indicate, it is inferred that the Co diffusion from the substrate surface to the atmosphere still exists at high substrate temperatures, which together with the Co diffusion from the inside to the surface of the substrate constitute a dynamic balance system, in which the latter is believed to dominate.

7) With the growing of the diamond films on the pretreated specimens, the Co diffusion from the film−substrate interface to the surface of as-deposited diamond film gradually becomes weaker and even disappears, which is attributed to the barrier action of the well-grown diamond crystals.

4 Conclusions

1) Relatively high substrate temperatures (800 and 950 °C) will induce the increment of the Co content on pretreated substrate surfaces, and thus have detrimental effects on the nucleation rate and the film quality. For the untreated specimens, at an extremely high substrate temperature (950 °C), the Co contents on substrate surfaces apparently reduce, which is attributed to the diffusion of the Co element to the atmosphere.

2) Under the heating condition, the diffusion of the Co element from the untreated substrate surface to the atmosphere is much more clear. In the actual deposition process of the diamond film, a dynamic balance system forms, including the Co diffusion from the inside to the

surface of the substrate, and the Co diffusion from the substrate surface to the atmosphere, but the former dominates.

3) The diffusion of the Co element from the inside to the surface of the substrate becomes much rapider when reducing *D*, and under the condition of the present study, the appropriate *D* is 8−9 μm.

4) The Co diffusion from the interface to the surface gradually becomes weaker and even disappears with the increase of the growth duration, as a result of the barrier action of the well-grown diamond crystals. For the pretreated WC−Co specimen with relatively high original Co content, under the same *D*, the Co content gradient from the inside to the surface of the substrate is larger. So, during the nucleation or growth process, the corresponding Co diffusion is rapider, which cannot inhibit the diamond nucleation but also slow the film growth and deteriorate the film quality close to the film−substrate interface.

5) For the Co-rich WC−Co substrates, on the premise that the toughness of the diamond coated components can meet the requirements of the applications, the *D* should be as large as possible (8−9 μm), and some additional pretreatment technologies are essential.

References

[1] UHLMANN E, LACHMUND U, BRUCHER M. Wear behavior of HFCVD-diamond coated carbide and ceramic tools [J]. Surface and Coatings Technology, 2000, 131: 395−399.

[2] SUN F H, MA Y P, SHEN B, ZHANG Z M, CHEN M. Fabrication and application of nano-microcrystalline composite diamond films on the interior hole surfaces of Co cemented tungsten carbide substrates [J]. Diamond and Related Materials, 2009, 18: 276−282.

[3] WANG X, SHEN B, SUN F. CVD diamond films as wear-resistant coatings for relief valve components in the coal liquefaction equipment [J]. Solid State Phenomena, 2011, 175: 219−225.

[4] CAPPELI E, PINZARI F, ASCARELLI P, RIGHINI G. Diamond nucleation and growth on different cutting tool materials: Influence of substrate pre-treatments [J]. Diamond and Related Materials, 1996, 5: 292−298.

[5] SAHOO B, CHATTOPADHYAY A K. On effectiveness of various surface treatments on adhesion of HF-CVD diamond coating to tungsten carbide inserts [J]. Diamond and Related Materials, 2002, 11: 1660−1669.

[6] SARANGI S K, CHATTOPADHYAY A, CHATTOPADHYAY A K. Effect of pretreatment methods and chamber pressure on morphology, quality and adhesion of HFCVD diamond coating on cemented carbide inserts [J]. Applied Surface Science, 2008, 254: 3721−3733.

[7] PETERS M G, CUMMINGS R H. Methods for coating adherent diamond films on cemented tungsten carbide substrates: US Patent, 5236740 [P]. 1993.

[8] SINGH R K, GILBERT D R, FITZ-GERALD J, HARKNESS S, LEE D G. Engineered interfaces for adherent diamond coatings on large thermal-expansion coefficient mismatched substrates [J]. Science, 1996, 272: 396−398.

[9] SAITO Y, SATO K, MATUDA S, KOINUMA H. Application of diamond films from CO-H2 plasma to tool blade coating [J]. Journal of Materials Science, 1991, 26: 2937−2940.

[10] TONSHOFF H K, MOHLFELD A, WINKLER J. Mechanical pretreatment for improved adhesion of diamond coatings [J]. Surface and Coatings Technology, 1999, 116−119: 440−446.

[11] ULLRAM S, HAUBNER R. Temperature pre-treatments of hardmetal substrates to reduce the cobalt content and improve diamond deposition [J]. Diamond and Related Materials, 2006, 15: 994−999.

[12] SHIBUKI K, YAGI M, SAIJO K, TAKATSU S. Adhesion strength of diamond films on cemented carbide substrates [J]. Surface and Coatings Technology, 1988, 36: 295−302.

[13] LU F X, TANG W Z, TONG Y M, MIAO J Q, HE L F, LI C M, ChEN G C. Novel pretreatment of hard metal substrate for better performance of diamond coated cutting tools [J]. Diamond and Related Materials, 2006, 15: 2039−2045.

[14] WEI Q P, YU Z M, ASHFOLD M N R, YE J, MA L. Synthesis of micro- or nano-crystalline diamond films on WC−Co substrates with various pretreatments by hot filament chemical vapor deposition [J]. Applied Surface Science, 2010, 256: 4357−4364.

[15] WANG L, LEI X, SHEN B, SUN F, ZHANG Z. Tribological properties and cutting performance of boron and silicon doped diamond films on Co-cemented tungsten carbide inserts [J]. Diamond and Related Materials, 2013, 33: 54−62.

[16] SATO T, HOSOKAWA Y, ITO S, AKASHI K. Plasma carbonitriding of cemented carbide substrate as an effective pretreatment process for diamond CVD [J]. Surface and Coatings Technology, 1999, 112: 189−193.

[17] SARANGI S K, CHATTOPADHAY A, CHATTOPADHYAY A K. Effect of pretreatment, seeding and interlayer on nucleation and growth of HFCVD diamond films on cemented carbide tools [J]. International Journal of Refractory Metals and Hard Materials, 2008, 26: 220−231.

[18] HEI H, MA J, LI X, YU S, TANG B, SHEN Y, TANG W. Preparation and performance of chemical vapor deposition diamond coatings synthesized onto the cemented carbide micro-end mills with a SiC interlayer [J]. Surface and Coatings Technology, 2015, 261: 272−277.

[19] XU F, XU J H, YUEN M F, ZHENG L, LU W Z, ZUO D W. Adhesion improvement of diamond coatings on cemented carbide with high cobalt content using PVD interlayer [J]. Diamond and Related Materials, 2013, 34: 70−75.

[20] KUPP E R, DRAWL W R, SPEAR K E. Interlayers for diamond-coated cutting tools [J]. Surface and Coatings Technology, 1994, 68: 378−383.

[21] MARTINI C, MORRI A. Face milling of the EN AB-43300 aluminum alloy by PVD- and CVD-coated cemented carbide inserts [J]. International Journal of Refractory Metals and Hard Materials, 2011, 29: 662−673.

[22] ALMEIDA F A, SACRAMENTO J, OLIVERIRA F J, SILVA R F. Micro- and nano-crystalline CVD diamond coated tools in the turning of EDM graphite [J]. Surface and Coatings Technology, 2008, 203: 271−276.

[23] ALMEIDA F A, CARRAPICHANO J M, FERNANDES A J S, SACRAMENTO J, SILVA R F, OLIVEIRA F J. Nanocrystalline CVD diamond coatings for drilling of WC−Co parts [J]. International Journal of Refractory Metals and Hard Materials, 2011, 29: 618−622.

[24] YAL S H, SU Y L, KAO W H, CHENG K W, SU C T. Nanolayer CrNx/WNy coatings used on micro drills for machining of printed circuit boards [J]. Journal of Materials Processing Technology, 2010, 210: 660−668.

[25] ZHANG J, WANG X, SHEN B, SUN F. Effect of boron and silicon doping on improving the cutting performance of CVD diamond coated cutting tools in machining CFRP [J]. International Journal of Refractory Metals & Hard Materials, 2013, 41: 285−292.

[26] SCHAFER L, HOFER M, KROGER R. The versatility of

hot-filament activated chemical vapor deposition [J]. Thin Solid Films, 2006, 515: 1017−1024.
[27] FENG J, XIE Y N, LI Z, WU X Z, LI J G, MEI J, YU Z M, WEI Q P. Microscopic mechanical characteristics analysis of ultrananocrystalline diamond films [J]. Transactions of Nonferrous Metals Society of China, 2015, 25: 3291−3296.
[28] WEI Q P, YU Z M, MA L, YIN D F, YE J. The effects of temperature on nanocrystalline diamond films deposited on WC−13wt.%Co substrate with W−C gradient layer [J]. Applied Surface Science, 2009, 256: 1322−1328.
[29] SEIN H, AHMED W, REGO C. Application of diamond coatings onto small dental tools [J]. Diamond and Related Materials, 2002, 11: 731−735.
[30] DONNET J B, PAULMIER D, OULANTI H, LE HUU T. Diffusion of cobalt in diamond films synthesized by combustion flame method [J]. Carbon, 2004, 42: 2215−2221.
[31] CABRAL G, ALI N, TITUS E, GRACIO J. Cobalt diffusion in different microstructured WC−Co substrates during diamond chemical vapor deposition [J]. Journal of Phase Equilibria and Diffusion, 2005, 26: 411−416.
[32] PARK B S, BAIK Y J, LEE K R, EUN K Y, KIM D H. Behaviour of Co binder phase during diamond deposition on WC−Co substrate [J]. Diamond and Related Materials, 1993, 2: 910−917.
[33] POLINI R, LE NORMAND F, MARCHESELLI G, TRAVERSA E. Early stages of diamond-film formation on cobalt-cemented tungsten carbide [J]. Journal of the American Ceramic Society, 1999, 82: 1429−1435.
[34] MEHLMANN A K, FAYER A, DIRNFELD S F, AVIGAL Y, PORATH R, KOCHMAN A. Nucleation and growth of diamond on cemented carbides by hot-filament chemical vapor deposition [J]. Diamond and Related Materials, 1993, 2: 317−322.
[35] ZHANG J, ZHANG T, WANG X, SHEN B, SUN F. Simulation and experimental studies on substrate temperature and gas density field in HFCVD diamond films growth on WC−Co drill tools [J]. Surface Review and Letters, 2013, 20: 1350020.
[36] DEUERLER F, van den BERG H, TABERSKY R, FREUNDLIEB A, PIES M, BUCK V. Pretreatment of substrate surface for improved adhesion of diamond films on hard metal cutting tools [J]. Diamond and Related Materials, 1996, 5: 1478−1489.
[37] GUO L, CHEN G. High-quality diamond film deposition on a titanium substrate using the hot-filament chemical vapor deposition method [J]. Diamond and Related Materials, 2007, 16: 1530−1540.
[38] HAYASHI Y, DRAWL W, MESSIER R. Temperature dependence of nucleation density of chemical vapor deposition diamond [J]. Japanese Journal of Applied Physics, 1992, 31: 193−196.
[39] ABREU C S, OLIVERIRA F J, BELMONTE M, FERNANDES A J S, GOMES J R, SILVA R F. CVD diamond coated silicon nitride self-mated systems: Tribological behavior under high loads [J]. Tribology Letters, 2006, 21: 141−151.
[40] LEI X, SHEN B, CHENG L, SUN F, CHEN M. Influence of pretreatment and deposition parameters on the properties and cutting performance of NCD coated PCB micro drills [J]. International Journal of Refractory Metals & Hard Materials, 2014, 43: 30−41.
[41] RAGHUVEER M S, YOGANAND S N, JAGANNADHAM K, LEMASTER R L, BAILEY J. Improved CVD diamond coatings on WC−Co tool substrates [J]. Wear, 2002, 253: 1194−1206.

金刚石形核及薄膜生长过程中不同钴含量 WC−Co 基体中的钴演变

王新昶[1]，王成川[1]，何为凯[2]，孙方宏[1]

1. 上海交通大学 机械与动力工程学院 机械系统与振动国家重点实验室，上海 200240；
2. 济南大学 物理科学与技术学院，济南 250022

摘 要：在具有不同钴含量(6%，10%和 12%，质量分数)的硬质合金样品上进行系统试验。基于 XPS 和 EDX 检测方法，采用正交试验方法证明了酸浓度、酸处理时间和原始钴含量对去钴深度有显著影响。在此基础上，研究形核、纯氢气氛围加热及生长试验条件下基体温度、原始钴含量及去钴深度对钴演变的影响规律。得到金刚石薄膜涂层器件制备全过程中钴元素的演变机理，为 WC−Co 基体表面、尤其是高钴含量 WC−Co 基体表面高质量金刚石薄膜的沉积提供理论依据。结果表明：高钴基体通常表现出较快的钴扩散速度；较高的基体温度会促进预处理基体中的钴扩散，但是在未处理基体中却表现出钴刻蚀作用；对于 WC−12%Co 基体，较为合适的预处理深度为 8−9 μm。

关键词：HFCVD 金刚石薄膜；WC−Co；Murakami-酸溶液预处理；钴含量；钴演变

(Edited by Xiang-qun LI)